Title
Variable ageing and storage of dissolved organic components in the open ocean

Journal
Nature, 430(7002)

ISSN
0028-0836

Authors
Loh, Ai Ning
Bauer, James E
Druffel, Ellen RM

Publication Date
2004-08-01

DOI
10.1038/nature02780

for 30 min on ice. Alternatively, the splenocytes were treated with Phos–Flag *ex vivo* and then FITC–anti-Flag as described above. All cells were analysed by flow cytometry.

Received 12 May; accepted 25 June 2004; doi:10.1038/nature02791.

1. Keppler, O. T., Horstkorte, R., Pawlita, M., Schmidts, C. & Reutter, W. Biochemical engineering of the *N*-acyl side chain of sialic acid: biological implications. *Glycobiology* **11,** 11R–18R (2001).
2. Dube, D. H. & Bertozzi, C. R. Metabolic oligosaccharide engineering as a tool for glycobiology. *Curr. Opin. Chem. Biol.* **7,** 616–625 (2003).
3. Buttner, B. *et al.* Biochemical engineering of cell surface sialic acids stimulates axonal growth. *J. Neurosci.* **22,** 8869–8875 (2002).
4. Keppler, O. T. *et al.* Biosynthetic modulation of sialic acid-dependent virus-receptor interactions of two primate polyoma viruses. *J. Biol. Chem.* **270,** 1308–1314 (1995).
5. Charter, N. W., Mahal, L. K., Koshland, D. E. & Bertozzi, C. R. Differential effects of unnatural sialic acids on the polysialylation of the neural cell adhesion molecule and neuronal behavior. *J. Biol. Chem.* **277,** 9255–9261 (2002).
6. Mahal, L. K., Yarema, K. J. & Bertozzi, C. R. Engineering chemical reactivity on cell surfaces through oligosaccharide biosynthesis. *Science* **276,** 1125–1128 (1997).
7. Saxon, E. & Bertozzi, C. R. Cell surface engineering by a modified Staudinger reaction. *Science* **287,** 2007–2010 (2000).
8. Kayser, H. *et al.* Biosynthesis of a nonphysiological sialic acid in different rat organs, using *N*-propanoyl-D-hexosamines as precursors. *J. Biol. Chem.* **267,** 16934–16938 (1992).
9. Saxon, E. *et al.* Investigating cellular metabolism of synthetic azidosugars with the Staudinger ligation. *J. Am. Chem. Soc.* **124,** 14893–14902 (2002).
10. Hang, H. C., Yu, C., Kato, D. L. & Bertozzi, C. R. A metabolic labeling approach toward proteomic analysis of mucin-type O-linked glycosylation. *Proc. Natl Acad. Sci. USA* **100,** 14846–14851 (2003).
11. Vocadlo, D. J., Hang, H. C., Kim, E. J., Hanover, J. A. & Bertozzi, C. R. A chemical approach for identifying *O*-GlcNAc-modified proteins in cells. *Proc. Natl Acad. Sci. USA* **100,** 9116–9121 (2003).
12. Kohn, M. & Breinbauer, R. The Staudinger ligation—A gift to chemical biology. *Angew. Chem. Int. Edn Engl.* **43,** 3106–3116 (2004).
13. Ovaa, H. *et al.* Chemistry in living cells: Detection of active proteasomes by a two-step labeling strategy. *Angew. Chem. Int. Edn Engl.* **42,** 3626–3629 (2003).
14. Kim, Y. J. & Varki, A. Perspectives on the significance of altered glycosylation of glycoproteins in cancer. *Glycoconj. J.* **14,** 569–576 (1997).
15. Fukuda, M. Possible roles of tumor-associated carbohydrate antigens. *Cancer Res.* **56,** 2237–2244 (1996).
16. Renkonen, J., Tynninen, O., Hayry, P., Paavonen, T. & Renkonen, R. Glycosylation might provide endothelial zip codes for organ-specific leukocyte traffic into inflammatory sites. *Am. J. Pathol.* **161,** 543–550 (2002).
17. Luchansky, S. J. *et al.* Constructing azide-labeled cell surfaces using polysaccharide biosynthetic pathways. *Methods Enzymol.* **362,** 249–272 (2003).
18. Kavarana, M. J., Kovaleva, E. G., Creighton, D. J., Wollman, M. B. & Eiseman, J. L. Mechanism-based competitive inhibitors of glyoxalase I: Intracellular delivery, *in vitro* antitumor activities, and stabilities in human serum and mouse serum. *J. Med. Chem.* **42,** 221–228 (1999).
19. Morton, C. L. *et al.* Activation of CPT-11 in mice: Identification and analysis of a highly effective plasma esterase. *Cancer Res.* **60,** 4206–4210 (2000).
20. Soares, E. R. Identification of a new allele of Es-I segregating in an inbred strain of mice. *Biochem. Genet.* **17,** 577–583 (1979).
21. Kiick, K. L., Saxon, E., Tirrell, D. A. & Bertozzi, C. R. Incorporation of azides into recombinant proteins for chemoselective modification by the Staudinger ligation. *Proc. Natl Acad. Sci. USA* **99,** 19–24 (2002).
22. Stasche, R. *et al.* A bifunctional enzyme catalyzes the first two steps in *N*-acetylneuraminic acid biosynthesis of rat liver—Molecular cloning and functional expression of UDP-*N*-acetyl-glucosamine 2-epimerase/*N*-acetylmannosamine kinase. *J. Biol. Chem.* **272,** 24319–24324 (1997).
23. Luchansky, S. J., Argade, S., Hayes, B. K. & Bertozzi, C. R. Metabolic functionalization of recombinant glycoproteins. *Biochemistry* (in the press).
24. Shaw, C. F. Gold-based therapeutic agents. *Chem. Rev.* **99,** 2589–2600 (1999).
25. Jurisson, S. S. & Lydon, J. D. Potential technetium small molecule radiopharmaceuticals. *Chem. Rev.* **99,** 2205–2218 (1999).
26. Codington, J. F., Klein, G., Silber, C., Linsley, K. B. & Jeanloz, R. W. Variations in the sialic acid compositions in glycoproteins of mouse ascites tumor-cell surfaces. *Biochemistry* **18,** 2145–2149 (1979).
27. Sell, S. Cancer-associated carbohydrates identified by monoclonal antibodies. *Hum. Pathol.* **21,** 1003–1019 (1990).
28. Kolb, H. C. & Sharpless, K. B. The growing impact of click chemistry on drug discovery. *Drug Discov. Today* **8,** 1128–1137 (2003).
29. Martin, D. C., Fowlkes, J. L., Babic, B. & Khokha, R. Insulin-like growth factor II signaling in neoplastic proliferation is blocked by transgenic expression of the metalloproteinase inhibitor TIMP-1. *J. Cell Biol.* **146,** 881–892 (1999).
30. Reichner, J. S., Whiteheart, S. W. & Hart, G. W. Intracellular trafficking of cell surface sialoglycoconjugates. *J. Biol. Chem.* **263,** 16316–16326 (1988).

Supplementary Information accompanies the paper on **www.nature.com/nature**.

Acknowledgements We thank A. Jamieson, S. Luchansky, H. Hang and P. Drake for discussions. J.A.P. was supported by a HHMI Predoctoral Fellowship and D.H.D. was supported by a National Science Foundation Predoctoral Fellowship. Sialic acid analysis was performed by the UCSD GRTC Glycotechnology Core Resource. This work was supported by grants from Johnson & Johnson (Focused Giving Grant), the Mizutani Foundation for Glycoscience, the US Department of Energy and the National Institutes of Health.

Competing interests statement The authors declare that they have no competing financial interests.

Correspondence and requests for materials should be addressed to C.R.B. (crb@berkeley.edu).

Variable ageing and storage of dissolved organic components in the open ocean

Ai Ning Loh[1]*, James E. Bauer[1] & Ellen R. M. Druffel[2]

[1]*School of Marine Science, College of William and Mary, PO Box 1346, Gloucester Point, Virginia 23062, USA*
[2]*Department of Earth System Science, University of California at Irvine, 3224 Croul Hall, Irvine, California 92697-3100, USA*

* Present address: Division of Ecological Studies, College of Arts and Sciences, Florida Gulf Coast University, 10501 FGCU Boulevard South, Fort Myers, Florida 33965, USA

Seawater dissolved organic matter (DOM) is the largest reservoir of exchangeable organic carbon in the ocean, comparable in quantity to atmospheric carbon dioxide[1,2]. The composition, turnover times and fate of all but a few planktonic constituents of this material are, however, largely unknown[3,4]. Models of ocean carbon cycling are thus limited by the need for information on temporal scales of carbon storage in DOM subcomponents, produced via the 'biological pump', relative to their recycling by bacteria[3,4]. Here we show that carbohydrate- and protein-like substances in the open Atlantic and Pacific oceans, though often significantly aged, comprise younger fractions of the DOM, whereas dissolved lipophilic material exhibits up to ~90 per cent fossil character. In contrast to the millennial mean ages of DOM observed throughout the water column, weighted mean turnover times of DOM in the surface ocean are only decadal in magnitude. An observed size–age continuum further demonstrates that small dissolved molecules are the most highly aged forms of organic matter, cycling much more slowly than larger, younger dissolved and particulate precursors, and directly links oceanic organic matter age and size with reactivity[3,5].

Seawater DOM consists of analytically identifiable biochemicals such as carbohydrates, proteins and lipids, as well as operationally defined and long-lived geomacromolecules (for example, humic and fulvic substances[5,6]). In order to resolve some of the key details of DOM sources and cycling in the oceans, major organic components were extracted from high-molecular-weight ultrafiltered DOM[5] (DOM_{HMW}, >1,000 daltons) collected from 1,000–3,000 l of sea water, and analysed for both $\Delta^{14}C$ and $\delta^{13}C$ isotopic signatures. Samples were collected from surface mixed-layer (3–20 m), mesopelagic oxygen-minimum (850–900 m), and abyssal (1,500–1,800 m) depths in the central North Pacific (June 1999) and the Sargasso Sea region of the North Atlantic (June 2000) oligotrophic ocean gyres. The contributions of solvent-extractable lipids, protein-like and carbohydrate-like organic matter (OM), as well as different molecular-weight fractions, to the overall age structure of seawater DOM, were thus established.

By far the most highly aged DOM component was the lipid extract (6.4–17.1 kyr before present, BP; Table 1), with ^{14}C ages in the deep Pacific representing the greatest yet observed for any component of seawater OM. The lipid extract was considerably older by ~5–13 kyr than the total DOM_{HMW} and unfractionated, bulk DOM (ΣDOM) pools (Tables 1 and 2; Fig. 1a). Furthermore, at all mesopelagic and abyssal depths, the lipid extract and DOM_{HMW} were older in the Pacific than in the Atlantic, similar to the ocean–ocean offsets observed for ΣDOM[6,7] (Table 1) and presumably due to cumulative ageing during deep water-mass transit[8]. Conversely, mixed-layer lipid extract, DOM_{HMW} and ΣDOM were all older in the Atlantic than in the Pacific (Tables 1 and 2), suggesting possible aged North American continental or atmospheric inputs there[9]. The highly $\delta^{13}C$-depleted signatures of lipid extracts (Table 1, Fig. 1b) are consistent with isotopic fractionations during cellular lipid

synthesis[10]. Thus, these fossil dissolved lipids arise either from extensive ageing within the oceans, with concomitant recycling over many ocean circulation times[8], or from inputs of one or more pre-aged lipophilic precursors[11]. Concurrent elemental ratios (Table 2) and lipid biomarker data[12] of total DOM_{HMW} suggest, however, that the lipid extract may be dominated by planktonic, rather than petrogenic, material.

Dissolved protein-like and carbohydrate-like fractions were similar in ^{14}C age, ranging from modern to ~3–4 kyr BP (Table 1). Modern to near-modern ages in surface waters indicate that both fractions are derived from recent, post-bomb (that is, after ~1955) marine production, and contain little aged or recycled material. In deeper waters, however, these components, which are quite reactive in surface waters[4], are deduced to have escaped degradation over many ocean circulation times[8] and to have aged extensively. The protein- and carbohydrate-like components were younger by as much as ~13–14 kyr compared to the corresponding lipid extract (Table 1), and by as much as ~1 kyr (Fig. 1a) compared to DOM_{HMW}, supporting the contention that 'old' seawater ΣDOM[1,6,7] is actually composed of components having a spectrum of ages and reactivities. Transport-based ageing of protein- and carbohydrate-like DOM is also suggested at mesopelagic and abyssal depths (Table 1), similar to the ΣDOM[6,7], total DOM_{HMW} and lipid extract (Tables 1 and 2).

Dissolved forms of all three major organic fractions were significantly older than their particulate counterparts[13,14] (Fig. 2). Dissolved lipid extracts were ~6–17 kyr older than lipid extracts of sinking particulate OM (POM; 3,500 m depth)[13,14], suggesting that dissolved and particulate lipids cycle on dramatically different timescales or arise from dissimilar sources. The latter possibility is supported by correspondingly lower $\delta^{13}C$ of dissolved lipids (about −29 to −28‰; Table 1) compared to particulate and sedimentary lipids (−25‰ to −22‰; refs 13, 14; Fig. 2). Alternatively, particulate lipids may contain both a highly aged component, similar to the dissolved pool, and a recently derived component from contemporary marine production[15], accounting for their intermediate ages. Deep dissolved protein- and carbohydrate-like fractions were also significantly older by ~3–4 kyr than particulate forms[13,14], whereas the relative abundances of these two fractions are reversed in the dissolved (Table 1) compared to particulate phases[13,14], suggesting dissimilar sources or preservation. Therefore, although the dissolved fractions are far more abundant, they are also far longer-lived

Table 1 **Isotopic signatures of organic fractions contained in seawater DOM_{HMW}**

Depth	LE			PL			CL			MUC		
	%*	$\Delta^{14}C$ (‰)	$\delta^{13}C$ (‰)	%*	$\Delta^{14}C$ (‰)	$\delta^{13}C$ (‰)	%*	$\Delta^{14}C$ (‰)	$\delta^{13}C$ (‰)	%†	$\Delta^{14}C$ (‰)	$\delta^{13}C$ (‰)
Atlantic												
3 m	0.1	−637 (8,140)§	−28‡	13.3	2 (modern)	−21.2	47.5	13 (modern)	−21.5	39.1	−28 (230)	−22.3
850 m	0.3	−730 (10,520)	−28.1	17.1	−190 (1,690)	−20.4	38.9	−228 (2,080)	−20.4	43.7	−336 (3,292)	−21.7
1,500 m	0.2	−830 (14,250)	−28‡	22.9	−215 (1,950)	−20.8	33.8	−309 (2,969)	−21‡	43.0	−246 (2,271)	−21.5
Pacific												
20 m	0.3	−551 (6,430)	−27.6	19.0	−21 (170)	−21‡	35.9	7 (modern)	−21.4	44.9	−199 (1,780)	−22.3
900 m	0.3	−864 (16,010)	−29.4	15.4	−279 (2,620)	−21.0	27.7	−302 (2,890)	−20.4	56.7	−444 (4,720)	−22.1
1,800 m	0.3	−881 (17,100)	−28‡	16.9	−332 (3,240)	−20.8	41.1	−406 (4,180)	−20.3	41.7	−499 (5,550)	−22.3

*% of each organic fraction in DOM_{HMW}, based on C equivalents measured after combustion to CO_2.
†%MUC = 100 − (%LE + %PL + %CL). Isotopic signatures of MUC were estimated by isotopic mass balance, as: $X_{MUC} = (X_{HMW} - f_{LE}X_{LE} - f_{PL}X_{PL} - f_{CL}X_{CL})/f_{MUC}$, where X is the $\Delta^{14}C$ or $\delta^{13}C$ signature of each organic fraction, f is the relative contribution of each to the total DOM_{HMW} pool, and $f_{LE} + f_{PL} + f_{CL} + f_{MUC} = 1.0$.
‡Assumed from average of all observed values in that group for purposes of inclusion of $\Delta^{14}C$-$\delta^{13}C$ pair in Fig. 2.
§Values in parentheses are ^{14}C ages in yr BP calculated from $\Delta^{14}C$ values as: $\text{Age (yr BP)} = -8,033 \ln(1 + \frac{\Delta^{14}C}{1,000})$ where yr BP indicate years before 1950, prior to thermonuclear weapons testing[27]. As $\Delta^{14}C$ values were not reservoir-corrected, all ages are not true calendar ages.

Table 2 **Isotopic and elemental characteristics of seawater DOM size classes**

Depth	ΣDOM*		DOM_{HMW}†		DOM_{LMW}‡		DOM_{HMW}		
	$\Delta^{14}C$ (‰)	$\delta^{13}C$ (‰)	$\Delta^{14}C$ (‰)	$\delta^{13}C$ (‰)	$\Delta^{14}C$ (‰)	$\delta^{13}C$ (‰)	C:N	C:P	N:P
Atlantic									
3 m	−238 (2,180)§	−21.3	−5 (40)	−21.8	−280 (2,640)	−21.2	14	353	25
850 m	−375 (3,780)	−21.2	−270 (2,528)	−21‖	−383 (3,885)	−21.2	14	268	19
1,500 m	−378 (3,810)	−20.8	−262 (2,440)	−21.2	−384 (3,890)	−20.8	14	196	14
Pacific									
20 m	−191 (1,700)	−21.2	−92 (780)	−21.8	−210 (1,890)	−21.1	15	280	19
900 m	−470 (5,100)	−20.8	−381 (3,850)	−21.5	−481 (5,260)	−20.7	14	284	21
1,800 m	−533 (6,120)	−21.2	−434 (4,570)	−21.3	−539 (6,220)	−21.2	14	256	18

*Unfractionated, bulk DOM values[6,7].
†High-molecular-weight DOM was 15–16% of ΣDOM in surface waters, and 5–11% in deeper waters based on C recoveries after ultrafiltration, diafiltration and lyophilisation. These recoveries are consistent with the range of recoveries reported in other studies[5,16,19].
‡Isotopic signatures of low-molecular-weight DOM, estimated by isotopic mass balance as: $X_{LMW} = (X_{\Sigma DOM} - f_{HMW}X_{HMW})/(1 - f_{HMW})$, where X is the $\Delta^{14}C$ or $\delta^{13}C$ value of each molecular weight fraction, f is the relative contribution of HMW and LMW material to ΣDOM, and $f_{HMW} + f_{LMW} = 1.0$.
§Values in parentheses are ^{14}C ages in yr BP calculated from $\Delta^{14}C$ values as in Table 1.
‖Assumed from average of all observed values in that group for purposes of inclusion of $\Delta^{14}C$-$\delta^{13}C$ pair in Fig. 2.

and are thus deduced to be less reactive to bacteria than the younger particulate fractions. Dissolved carbohydrates have further been found to contain specific sugars of modern ^{14}C age[16], indicating that even within a given organic fraction individual molecules may have unique cycling times, similar to findings for individual sedimentary lipids[11].

The highly modified, acid-insoluble fraction of DOM_{HMW} (analogous to the molecularly uncharacterized, MUC, component of OM[17]) was estimated to comprise 39–57% of DOM_{HMW} carbon (Table 1). These large amounts of MUC-like DOM and its estimated ages (0.2–5.6 kyr BP; Table 1) suggest that much of the ΣDOM is composed of structurally modified biopolymers and geomolecules[17], probably derived from combinations of diagenetically altered younger proteins and sugars and older lipid components. Based on their disparate $\Delta^{14}C$ and $\delta^{13}C$ signatures (Table 1, Fig. 2), however, the dissolved forms of MUC and lipid extract are unlikely to share a common origin as has been suggested for POM[14]. Instead, dissolved MUC in deep waters is isotopically more similar to, and thus may arise from, dissolved protein- and carbohydrate-like and humic materials[6] (Fig. 2), or from a precursor common to each. This is further supported by NMR studies demonstrating that DOM_{HMW} contains significant acyl polysaccharide, a carbohydrate-derived biopolymer[18].

Radiocarbon ages for total DOM_{HMW} ranged widely, from modern to 4.6 kyr BP (Table 2), and were younger than ΣDOM[1,6] from the Atlantic and Pacific (Table 2). Therefore, ΣDOM must by definition also contain an older, low-molecular-weight (LMW) component in order to balance the younger DOM_{HMW} (ref. 19; Table 2). In addition to being the oldest size fraction yet identified for seawater OM (~1.9–6.2 kyr BP), DOM_{LMW} is also the most abundant, comprising 77–95% of ΣDOM. The $\delta^{13}C$ signatures of this older LMW material further suggest that it arises directly from recycling of younger DOM_{HMW} (Table 2). Observations of old DOM_{LMW}, intermediate-aged DOM_{HMW}, and young POM[7,20] in the oceans reveal a pronounced size–age relationship among the major forms of seawater OM (Table 2; Fig. 2). The two main forms of POM (that is, sinking and suspended) consistently contain bomb ^{14}C ($\Delta^{14}C$ range: about −100‰ to +160‰ for suspended POM, and about −30‰ to +35‰ for sinking POM) throughout the Pacific and Atlantic water columns[7,20]. However, only surface DOM_{HMW} is similarly enriched, while LMW material contains no apparent bomb ^{14}C at any depth (Table 2; Fig. 2). That is, ^{14}C age increases consistently in the size sequence from sinking POM (the youngest, largest fraction), to suspended POM, to DOM_{HMW} and finally DOM_{LMW} (the oldest, smallest fraction; Fig. 2), and most probably arises from sequential hydrolysis, dissolution and/or degradation of larger forms of OM to successively smaller fractions. This also suggests that the relative rate of OM respiration slows as highly aged LMW material accumulates in the latter stages of degradation.

An important corollary of this size–age continuum is that it coincides with a previously observed OM size–reactivity continuum[3,5], ranging from structurally complex and recently produced sinking POM and DOM_{HMW} (most reactive to bacterial degradation) to structurally simple but highly reworked DOM_{LMW} (least reactive to bacterial degradation). The proposed size–age model for seawater OM is therefore consistent with higher utilization rates of DOM_{HMW} than DOM_{LMW} in oceanic and coastal waters[3,5] as well as with the presence of younger, presumably more reactive subcomponents[3,16] in DOM_{HMW} (Fig. 1a). Studies of ΣDOM degradation further support the presence of specific bioavailable subfractions of this large, heterogeneous pool[4]. Besides the ^{14}C evidence, highly elevated elemental ratios of DOM_{HMW} (Table 2; ref. 21) compared to recently produced 'Redfield' OM (C:N:P = ~106:16:1), together with the presence of bacterial fatty acids in oceanic DOM_{HMW} (ref. 12), further support the contention that dissolved components may have undergone extensive recycling compared to POM (Fig. 2). An alternative to the proposed size-dependent ageing model for seawater OM is that there exist one or

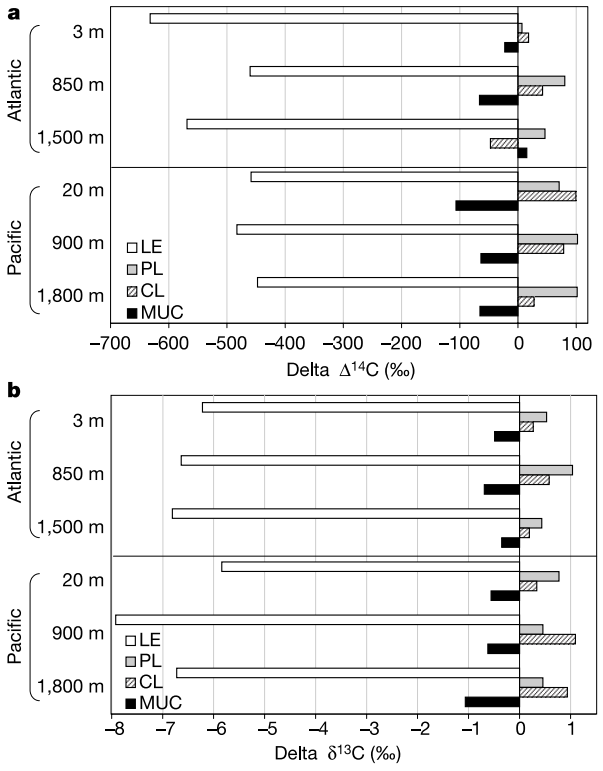

Figure 1 Isotopic signatures of dissolved organic fractions relative to DOM_{HMW}. **a**, Plotted for $\Delta^{14}C$ (as Delta $\Delta^{14}C$); and **b**, plotted for $\delta^{13}C$ (as Delta $\delta^{13}C$) for three depths each in the Sargasso Sea region of the North Atlantic and in the central North Pacific. LE, lipid-extract fraction; PL, protein-like fraction; CL, carbohydrate-like fraction; MUC, molecularly uncharacterized fraction. See Table 1 for assumed $\delta^{13}C$ values.

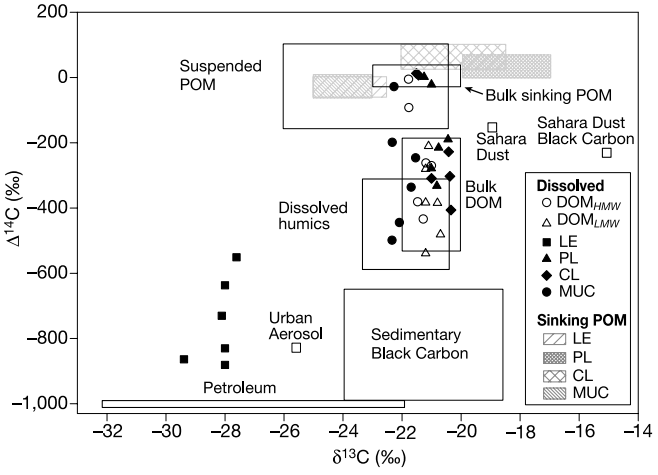

Figure 2 $\Delta^{14}C$ versus $\delta^{13}C$ for dissolved organic fractions, DOM_{HMW}, and DOM_{LMW}. Data from the present study are plotted as discrete points, along with ranges for potential sources of DOM in the North Atlantic and North Pacific oceans (boxes) compiled from the literature as follows: sinking POM[7]; suspended POM[20]; bulk DOM[6,7]; dissolved humic substances[6]; Sahara dust bulk organic matter and black carbon fraction[9]; urban aerosol[29]; North Pacific and Southern Ocean sedimentary black carbon[22]; and petroleum[30]. Shaded boxes show $\Delta^{14}C$ and $\delta^{13}C$ ranges for organic fractions isolated from sinking POM[13,14]. Abbreviations as in Fig. 1. See Tables 1 and 2 for assumed $\delta^{13}C$ values.

more allochthonous or autochthonous sources of pre-aged DOM in the oceans that are largely independent of plankton-dominated OM formation and degradation. While aged allochthonous sources of DOM such as submicrometre fossil black carbon[22] are probably minimal on the basis of the observed OM size–age distributions (Fig. 2), other 'pre-aged' inputs may include natural hydrocarbon seepage[23] in certain ocean regions and atmospheric deposition[9]. Soluble forms of seawater OM are further predicted to escape degradation and undergo ageing either within the deep ocean, or during surface-to-deep ocean transport, by mechanisms different from those such as sorptive preservation[24] identified for particulate and sedimentary forms.

Within the oceanic DOM pool, various organic and size fractions persist on radically different timescales (Tables 1 and 2). The turnover time (TOT) of undifferentiated bulk pools such as ΣDOM is equivalent to its ^{14}C age if substances in the bulk pool are uniform in age. However, the presence of discrete organic and size fractions having different ^{14}C ages (and therefore different rates of turnover) results in a weighted mean TOT that departs from the ΣDOM age[25]. On the basis of the heterogeneity in the organic and size fraction ages (Tables 1 and 2), the weighted mean TOT for surface ocean ΣDOM is estimated to be ~60–90 yr, increasing to ~3,700–6,000 yr in Atlantic and Pacific deep waters, respectively (see Supplementary Table S1). Surface ocean differences between the weighted mean TOT (decadal) and ΣDOM ^{14}C ages (millennial) result from surface DOM being dominated by young protein- and carbohydrate-like fractions that are recycled rapidly compared to the balance of the DOM. This contrasts with deep waters, where ΣDOM ages and TOT converge owing to the uniform low reactivity and turnover of all subcomponents. □

Methods

Sample collection and organic fraction separation

Large-volume (1,000–3,000 l) water samples were collected using 30-l rosette-mounted Niskin bottles. Samples were pre-filtered (0.2-μm) and transferred to an Amicon DC-10L tangential flow ultrafiltration system equipped with spiral wound filter cartridges with a 1,000 dalton molecular-weight cut-off. Samples were reduced to ~1 l and frozen until processing. For analyses, samples were thawed, diafiltered to remove salts, and lyophilised, followed by sequential extraction for solvent-extractable lipids, protein-like and carbohydrate-like organic fractions. Total lipids were extracted from the lyophilised sample using a modified Bligh-Dyer extraction with dichloromethane:methanol (2:1 v/v) and a Dionex accelerated solvent extractor[12]. Residue from the lipid extraction was divided by weight into two portions for protein-like and carbohydrate-like extraction and isotopic analyses (adapted from ref. 13). One portion was hydrolysed (6 N HCl at 100 °C for 19 h) and eluted with 1.5 N NH_4OH through a cation exchange column to trap the protein-like fraction. The other portion was hydrolysed for the carbohydrate-like fraction (72% H_2SO_4 for 2 h, then 0.6 M H_2SO_4 at 100 °C for 2 h). The solution was neutralized with $Ba(OH)_2$ $8H_2O$, adjusted to pH 6–7 with 1.5 N NH_4OH, and eluted with Nanopure water through a cation/anion exchange column to trap the carbohydrate-like fraction.

Concentrations and carbon isotope signatures of known standard compounds were measured before and after the extraction procedure to evaluate extraction efficiencies and potential isotopic fractionation caused by processing. The lipid standard was a mixture of a wax ester (C_{14} alcohol, C_{20} fatty acid), C_{19} alcohol, C_{19} fatty acid and androstanol. The amino-acid and sugar standards were L-leucine and D-glucose, respectively. Procedural blanks for protein and carbohydrate extraction methods were processed through the hydrolysis, neutralization, and elution steps using only the reagents. Blanks (2–3 each) needed to be combined to yield enough carbon for ^{14}C analyses. No lipid-extract blanks were measured isotopically because of their extremely low (≤1 μg) carbon yields. Mean standard recoveries were 76 ± 33% ($n = 4$) for the lipid extract, 66 ± 12% ($n = 4$) for the protein-like fraction and 93 ± 17% ($n = 4$) for the carbohydrate-like fraction.

Carbon isotope analyses

Total DOM_{HMW} and organic fractions (lipid extract, protein- and carbohydrate-like) were dried *in vacuo* and acidified with 1% H_3PO_4 overnight to remove any carbonates or dissolved inorganic carbon. Acidified samples were then dried *in vacuo* and the organic carbon oxidized to CO_2 at 850 °C in evacuated sealed quartz tubes containing CuO and Ag metal[26]. The CO_2 was purified and the yield quantified using a calibrated Baratron absolute pressure gauge (MKS Industries) on a vacuum extraction line. Samples were split into sealed Pyrex tubes for $\Delta^{14}C$ (~90% of total CO_2) and $\delta^{13}C$ (~10% of total CO_2) determinations. $\Delta^{14}C$ is defined here as the ‰ deviation of the $^{14}C/^{12}C$ ratio (^{13}C-normalized and corrected to AD 1950) for the sample relative to the $^{14}C/^{12}C$ ratio of the absolute international standard (95% of the AD 1950 activity of NBS Oxalic Acid I, normalized to $\delta^{13}C = -19‰$)[27]. Sample CO_2 for $\Delta^{14}C$ analyses was reduced to elemental graphite using H_2 over Co catalyst[28]. $\Delta^{14}C$ analyses were performed by accelerator mass spectrometry (AMS) and $\delta^{13}C$ measurements were made using a Finnigan Delta S isotope ratio mass spectrometer. The $\Delta^{14}C$ and $\delta^{13}C$ values of standard lipid, amino-acid and sugar compounds following extraction procedures were not significantly different from those of the pure compounds, indicating that both blank and fractionation effects were minimal. Errors ($\pm 1\sigma$) were considered to be the larger of either standard compound analyses or sample replicates ($n = 2$–3), and were ±9‰ for DOM_{HMW}, ±49‰ for the protein-like fraction and ±75‰ for the carbohydrate-like fraction for $\Delta^{14}C$ measurements, and ±0.9‰ for all $\delta^{13}C$ measurements. Owing to the small sample sizes, replicate lipid extractions were not possible. Errors for lipid-extract $\Delta^{14}C$ measurements were ±4–7‰ based on AMS analytical uncertainties. The ^{14}C ages of ΣDOM from this study were identical within measurement error to those determined previously at these two sites, and had not changed significantly over the 10–15 yr between the first and second occupations of the Pacific and Atlantic stations (J.E.B., unpublished data).

Weighted mean turnover time calculation

Weighted mean turnover times (TOT) for bulk DOM (ΣDOM) having non-homogeneous component ages were estimated by calculating first-order turnover rate constants for each individual DOM_{HMW} organic subcomponent (lipid extract, protein-like, carbohydrate-like and MUC fractions) and DOM_{LMW} as:

$$k_i = \frac{F_i}{A_i}$$

where k_i is the turnover rate constant in yr^{-1} for fraction i, F_i is the relative contribution of fraction i to the ΣDOM pool, and A_i is the ^{14}C age of fraction i (Tables 1 and 2, Supplementary Table S1). The weighted mean TOT[25] of ΣDOM is then calculated as:

$$\mathrm{TOT}_{\Sigma\mathrm{DOM}} = \frac{1}{\sum k_i}$$

Received 12 December 2003; accepted 24 June 2004; doi:10.1038/nature02780.

1. Williams, P. M. & Druffel, E. R. M. Radiocarbon in dissolved organic carbon in the central North Pacific Ocean. *Nature* **330,** 246–248 (1987).
2. Hedges, J. I. Global biogeochemical cycles: progress and problems. *Mar. Chem.* **39,** 67–93 (1992).
3. Amon, R. M. W. & Benner, R. Bacterial utilization of different size classes of dissolved organic matter. *Limnol. Oceanogr.* **41,** 41–51 (1996).
4. Carlson, C. A. in *Biogeochemistry of Marine Dissolved Organic Matter* (eds Hansell, D. A. & Carlson, C. A.) 91–151 (Academic, Orlando, USA, 2002).
5. Benner, R. in *Biogeochemistry of Marine Dissolved Organic Matter* (eds Hansell, D. A. & Carlson, C. A.) 59–90 (Academic, Orlando, USA, 2002).
6. Bauer, J. E., Williams, P. M. & Druffel, E. R. M. ^{14}C activity of dissolved organic carbon fractions in the north central Pacific and Sargasso Sea. *Nature* **357,** 667–670 (1992).
7. Druffel, E. R. M., Williams, P. M., Bauer, J. E. & Ertel, J. R. Cycling of dissolved and particulate organic matter in the open ocean. *J. Geophys. Res.* **97,** 15639–15659 (1992).
8. Stuiver, M., Quay, P. D. & Ostlund, H. G. Abyssal water ^{14}C distribution and the age of the world oceans. *Science* **219,** 849–851 (1983).
9. Eglinton, T. I. *et al.* Composition, age, and provenance of organic matter in NW African dust over the Atlantic Ocean. *Geochem. Geophys. Geosyst.* **3,** doi:10.1029/2001GC000269 (2002).
10. Goericke, R., Montoya, J. P. & Fry, B. in *Stable Isotopes in Ecology and Environmental Science* (eds Lajtha, K. & Michener, R. H.) 181–221 (Blackwell Scientific Publications, Oxford, UK, 1994).
11. Eglinton, T. I. *et al.* Variability in radiocarbon ages of individual organic compounds from marine sediments. *Science* **277,** 796–799 (1997).
12. Loh, A. N. *Chemical, Isotopic and Microbial Characterization of Dissolved and Particulate Organic Matter in Estuarine, Coastal and Open Ocean Systems*. Doctoral dissertation, College of William and Mary (2002).
13. Wang, X.-C., Druffel, E. R. M., Griffin, S., Lee, C. & Kashgarian, M. Radiocarbon studies of organic compound classes in plankton and sediment of the northeastern Pacific Ocean. *Geochim. Cosmochim. Acta* **62,** 1365–1378 (1998).
14. Hwang, J. & Druffel, E. R. M. Lipid-like material as the source of the uncharacterized organic carbon in the ocean? *Science* **299,** 881–884 (2003).
15. Wakeham, S. G., Hedges, J. I., Lee, C., Peterson, M. L. & Hernes, P. J. Compositions and transport of lipid biomarkers through the water column and surficial sediments of the equatorial Pacific Ocean. *Deep-Sea Res. II* **44,** 2131–2162 (1997).
16. Aluwihare, L. I., Repeta, D. J. & Chen, R. F. Chemical composition and cycling of dissolved organic matter in the mid-Atlantic bight. *Deep-Sea Res. II* **49,** 4421–4437 (2002).
17. Hedges, J. I. *et al.* The molecularly-uncharacterized component of nonliving organic matter in natural environments. *Org. Geochem.* **31,** 945–958 (2000).
18. Aluwihare, L. I., Repeta, D. J. & Chen, R. F. A major biopolymeric component to dissolved organic carbon in surface seawater. *Nature* **387,** 166–169 (1997).
19. Santschi, P. H. *et al.* Isotopic evidence for the contemporary origin of high-molecular weight organic matter in oceanic environments. *Geochim. Cosmochim. Acta* **59,** 625–631 (1995).
20. Druffel, E. R. M., Bauer, J. E., Griffin, S. & Hwang, J. Penetration of anthropogenic carbon into organic particles of the deep ocean. *Geophys. Res. Lett.* **30,** doi:10.1029/2003GL017423 (2003).
21. Clark, L. L., Ingall, E. D. & Benner, R. Marine phosphorus is selectively remineralised. *Nature* **393,** 426 (1998).
22. Masiello, C. A. & Druffel, E. R. M. Black carbon in deep-sea sediments. *Science* **280,** 1911–1913 (1998).
23. Wang, X.-C., Chen, R. F., Whelan, J. & Eglinton, L. Contribution of "old" carbon from natural marine hydrocarbon seeps to sedimentary and dissolved organic carbon pools in the Gulf of Mexico. *Geophys. Res. Lett.* **28,** 3313–3316 (2001).
24. Hedges, J. I. & Keil, R. G. Sedimentary organic matter preservation: an assessment and speculative synthesis. *Mar. Chem.* **49,** 81–115 (1995).
25. Trumbore, S. E. & Druffel, E. R. M. in *The Role of Nonliving Organic Matter in the Earth's Carbon Cycle* (eds Zepp, R. G. & Sonntag, Ch.) 7–22 (John Wiley & Sons, Chichester, UK, 1995).
26. Sofer, Z. Preparation of carbon dioxide for stable carbon isotope analysis of petroleum fractions. *Anal. Chem.* **52,** 1389–1391 (1980).

27. Stuiver, M. & Polach, H. A. Discussion: reporting of ^{14}C data. *Radiocarbon* **19,** 355–363 (1977).
28. Vogel, J. S., Southon, J. R. & Nelson, D. E. ^{14}C background levels in an AMS system. *Nucl. Instrum. Methods Phys. Res.* **29,** 50–56 (1987).
29. Masiello, C. A., Druffel, E. R. M. & Currie, L. A. Radiocarbon measurements of black carbon in aerosols and ocean sediments. *Geochim. Cosmochim. Acta* **66,** 1025–1036 (2002).
30. Whelan, J. K. & Thompson-Rizer, C. L. in *Organic Geochemistry: Principles and Applications* (eds Engel, M. H. & Macko, S. A.) 289–353 (Plenum, New York, USA, 1993).

Supplementary Information accompanies the paper on **www.nature.com/nature**.

Acknowledgements We thank E. Canuel, J. Hwang and S. Griffin for laboratory guidance during compound class extractions; M. Ederington-Hagy, E. Waterson and J. Southon for discussions on experiments; S. Griffin, R. Wilson, L. Delizo, C. Masiello, A. Grottoli and the captains and crews of RV *Melville* and RV *Knorr* for field assistance and logistical support; A. McNichol and colleagues at NOSAMS for $\Delta^{14}C$ measurements; E. Franks for $\delta^{13}C$ measurements; and R. Benner for comments that significantly improved this manuscript. This work was supported by the Chemical Oceanography Program of the US National Science Foundation.

Competing interests statement The authors declare that they have no competing financial interests.

Correspondence and requests for materials should be addressed to A.N.L. (anloh@fgcu.edu).

Impact of climate change on marine pelagic phenology and trophic mismatch

Martin Edwards & Anthony J. Richardson

Sir Alister Hardy Foundation for Ocean Science, The Laboratory, Citadel Hill, Plymouth PL1 2PB, UK

Phenology, the study of annually recurring life cycle events such as the timing of migrations and flowering, can provide particularly sensitive indicators of climate change[1]. Changes in phenology may be important to ecosystem function because the level of response to climate change may vary across functional groups and multiple trophic levels. The decoupling of phenological relationships will have important ramifications for trophic interactions, altering food-web structures and leading to eventual ecosystem-level changes. Temperate marine environments may be particularly vulnerable to these changes because the recruitment success of higher trophic levels is highly dependent on synchronization with pulsed planktonic production[2,3]. Using long-term data of 66 plankton taxa during the period from 1958 to 2002, we investigated whether climate warming signals[4] are emergent across all trophic levels and functional groups within an ecological community. Here we show that not only is the marine pelagic community responding to climate changes, but also that the level of response differs throughout the community and the seasonal cycle, leading to a mismatch between trophic levels and functional groups.

The vast majority of documented phenology studies relating seasonal shifts in biology to climate have come from terrestrial and limnological sources (see refs 5, 6). Furthermore, most studies have solely reported phenological changes for a single species and have not explored trophic and ecological interactions[7]. In this study we investigated changes in marine pelagic phenology in the North Sea across three trophic levels using five functional groups. The major functional groups included diatoms and dinoflagellates separately (primary producers); copepods (secondary producers); non-copepod holozooplankton (secondary and tertiary producers) and meroplankton including fish larvae (secondary and tertiary producers). Inter-annual changes in a measure of the timing of the seasonal peak throughout the whole pelagic production season (the central tendency; see Methods and Fig. 1a, b) were calculated using data from the Continuous Plankton Recorder (CPR)[8], one of the longest and most spatially extensive marine biological data sets in the world.

The *x* axis of Fig. 1c shows the timing of the seasonal peaks in 1958 of all 66 plankton taxa used in the analysis; this represents the classical view of succession in the temperate marine pelagic ecosystem. Using the linear slope of the time series of the timing of the seasonal peak, we calculated the change in timing of the seasonal cycle (in months) from 1958 to 2002 for each taxon (Fig. 1c; *y* axis). Substantial temporal modifications in seasonal successional peaks have occurred over the past few decades. In particular, seasonal peaks of meroplankton have moved significantly ($P < 0.0001$) forward (for example, the phylum Echinodermata has moved by 47 days (d)). By contrast, diatom peaks in spring and autumn have collectively remained relatively static, albeit with considerable

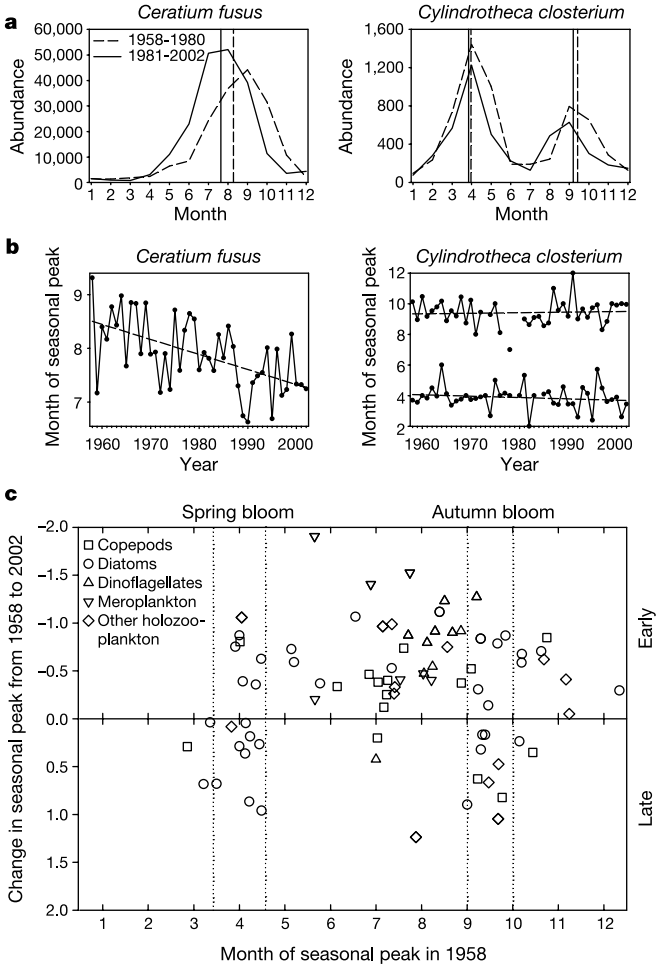

Figure 1 Changes in phenology throughout the pelagic season. **a**, Examples of seasonal cycles for two of the 66 taxa—the dinoflagellate *Ceratium fusus* and the diatom *Cylindrotheca closterium*—used in the analysis for the periods 1958–1980 and 1981–2002. The timing of the seasonal peaks, using the indicator of central tendency, is also shown. **b**, Inter-annual variability of the seasonal peak for the above two species from 1958 to 2002. **c**, The change in the timing of the seasonal peaks (in months) for the 66 taxa over the 45-yr period from 1958 to 2002 plotted against the timing of their seasonal peak in 1958. For each taxon, the linear regression in **b** was used to estimate the difference between the seasonal peak in 1958 and 2002. A negative difference between 1958 and 2002 indicates seasonal cycles are becoming earlier. Standard linear regression was considered appropriate because there was minimal autocorrelation (determined by the Durbin–Watson statistic) in the phenology time series.